Winding distribution effects on induction motor rotor fault diagnosis

C. Pezzani *, G. Bossio, C. De Angelo

Consejo Nacional de Investigaciones Científicas y Técnicas (CONICET), Argentina
Grupo de Electrónica Aplicada, Facultad de Ingeniería, Universidad Nacional de Río Cuarto, Ruta Nac. No. 36 km 601, X5804BYA Río Cuarto, Córdoba, Argentina

ARTICLE INFO

ABSTRACT

The sidebands around stator currents harmonics as a potential tool for supporting the diagnosis of rotor faults in induction motors are analyzed in this paper. The presence of broken bars introduces high frequency components in the machine currents spectrum in addition to the characteristic sidebands around the fundamental component. These additional components are due to the interaction between, rotor asymmetry and either the voltage harmonics, or winding distribution, or rotor slots. In particular, the components at frequencies near to fifth and seventh harmonics, produced by the interaction between the rotor faults and the harmonics of the spatial distribution of stator windings, are analyzed in this work. A multiple coupled circuit model of the induction motor is used to evaluate the sensitivity of these components for different stator winding configurations, load level, supply voltage conditions, and different number of broken bars. Simulation results showed that a particular analyzed component near to fifth harmonic depends mainly on fifth harmonic of winding distribution, which remains almost constant for most common distributions. Therefore, it is expected that this component should be found in most motors with broken bars. Finally, experimental laboratory results and two industrial cases that validate the analysis are presented.

© 2013 Elsevier Ltd. All rights reserved.

1. Introduction

Fault diagnosis in electrical machines, particularly induction motors (IM), has been a very active research area in recent times [1]. This is mainly due to the importance of IM in industrial production processes. The use of fault detection strategies in conjunction with a predictive maintenance program contributes to reduce unscheduled downtime [2,3].

Particularly the detection and correct diagnosis of broken bars in IM is a problem that has received special attention, despite it does not represent the fault of higher occurrence [2,3]. An important variety of strategies have been proposed as options to the already accepted mechanical vibration analysis. Fault detection techniques based on current and voltage measurement, powers and fluxes have proved efficiency in fault detection and diagnosis processes, not only for faults originated electromagnetically but also mechanically [3–9]. Among these strategies, the motor current signature analysis (MCSA) is the most widespread, due its simplicity and minimum number of required sensors [9–13]. Most of these strategies use the magnitude of the sidebands at the fundamental component $(1 \pm 2s)f_s$ as fault indicator, where s is the slip and f_s the supply frequency [10,13]. Suitable fault severity factors have been proposed

based on these sidebands [13]. However, the amplitude of these components not only depends on the fault severity, but it also depends on factors such as the load level and inertia of the motor-load set, among others [13–15]. Moreover, low-frequency oscillations in the load torque affect motor currents in a very similar way; that is, by introducing sidebands around the fundamental component. Situations of this nature hinder the correct quantification of the failure and may even induce false diagnosis [16].

Several proposals that pose solutions to these problems have been recently presented [17–21]. Some works propose strategies that require measurement of both, current and voltage [18], special sensors [19] or signals analysis during transient periods [21,22]. However, additional information to that provided by the components at frequencies $(1 \pm 2s)f_s$ can be extracted from the spectral analysis of a phase current, without resort to complex signals processing techniques nor additional sensors.

Particularly, the analysis of current components around high order harmonics has been proposed with the objective of improving rotor fault diagnosis [10,16]. In general, high frequency components are less sensitive to load oscillations due to the "filter" effect that inertia produces on oscillations. These high frequency components can be caused by the interaction between asymmetry on the rotor – due to broken bars – and either the harmonics due to supply voltage distortion or unbalances, or the spatial harmonics due to the stator windings distribution or the rotor slots harmonics (RSH) [23–27]. The use of the components due to supply voltage distortion or unbalance to generate rotor fault indicators was proposed and

* Corresponding author at: Grupo de Electrónica Aplicada, Facultad de Ingeniería, Universidad Nacional de Río Cuarto, Ruta Nac. No. 36 km 601, X5804BYA Río Cuarto, Córdoba, Argentina. Tel./fax: +54 358 4676598/4676255.
E-mail address: cpezzani@ing.unrc.edu.ar (C. Pezzani).

analyzed in [23]. Although these indicators are less sensitive to amplitude variations of voltage harmonics, it becomes necessary a certain degree of distortion. This can be quite easily achieved in inverter-fed motors. However, in motors supplied directly from the grid, it may not occur, even less in medium-voltage motors.

On the other hand, the use of components produced by a discrete distribution of the rotor (RSH) requires knowledge on some construction parameters such as the number of rotor bars and also an accurate estimate of the motor slip [24,25].

The non-sinusoidal distribution of windings produces spatial harmonics on magnetomotive force (*mmf*), mainly at frequencies given by $(6k \pm 1)f_s$, with $k = 1,2,\ldots$ The interaction between these spatial harmonics and rotor asymmetry produces characteristic components in the current spectrum of the IM [26]. The components at frequencies $(5 - 4s)f_s$, $(5 - 6s)f_s$, $(7 - 6s)f_s$ and $(7 - 8s)f_s$, located around 5th and 7th harmonics, are the most significant ones [27]. The use of these components as potential indicators of broken bars has been presented in [26,27]. However, for any fault indicator, a deep analysis of the influence of the motor operation conditions as well as other factors must be done in order to determine their effectiveness and applicability for fault detection and identification. A first analysis of the behavior of the components $(5 - 4s)f_s$ and $(7 - 6s)f_s$, for different number of broken bars, load inertia variations and supply voltage conditions was presented in [28]. From this analysis it was demonstrated, for a particular winding distribution, the usefulness of the components $(5 - 4s)f_s$ and $(7 - 6s)f_s$ to support the broken bars diagnosis.

In this paper a detailed analysis of the components $(5 - 4s)f_s$ and $(7 - 6s)f_s$ as indicators of broken bars in the IM is presented. A multiple coupled circuit model of the IM [29,30] is used to evaluate the sensitivity of these components for different winding configurations. Through numerical simulation, the amplitude of fault indicators is evaluated in terms of the winding distribution harmonics using the proposed model. The influence of voltage distortion, inertia and load level is also analyzed. Finally, several experimental laboratory results and two industrial cases that validate the analysis are presented.

2. Induction motor model

The components of interest for broken bar detection are produced by the interaction between the spatial harmonics of the stator winding distribution and rotor asymmetry due to broken bars. Therefore it becomes necessary use a model that allows considering different stator windings and rotor distributions. In this work, multiple-coupled circuit model proposed in [29] is used with this aim and the winding function method is employed for inductances calculation [30]. This approach allows considering the actual distribution of stator windings and rotor bars and facilitates the inductances calculation for different motors types or under fault conditions [31–33]. Saturation effects and eddy currents are neglected in this formulation and the rotor bars are supposed to be isolated. In addition, stator teeth and rotor slots are neglected since their effect hardly affects the components of interest [34]. The inclusion of saturation effects on induction and synchronous machines models using the WFA has been recently proposed in [38–40]. However, as will be later demonstrated in Section 5.1.2, this effect on the components of interest is negligible.

In general, the IM consists of m stator circuits and k rotor bars. The squirrel-cage rotor can be modeled as k identical equally spaced loops constituted by two consecutive bars plus a current loop on one of the end-rings (Fig. 1) [29]. In Fig. 1, r_e and L_e are the resistance and leakage inductance of the end-ring segment, respectively. r_b is the rotor bar resistance and L_b is the rotor bar leakage inductance.
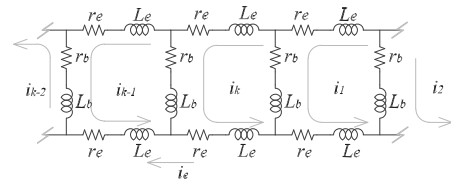

Fig. 1. Squirrel-cage equivalent circuit.

To calculate self and mutual inductances of the model, Modified Winding Function Approach [30] is used, which allows considering non-uniformity, both radial and axial, on windings and on the air–gap. This makes it possible to analyze the effects of winding distribution, skew and the variations in the air–gap due to either eccentricity or rotor and stator slots simultaneously. Mutual inductance between any two circuits, A and B of the motor can be calculated as,

$$L_{BA}(\theta_r) = \mu_0 r \int_0^{2\pi} \int_0^L n_B(\phi, z, \theta_r) N_A(\phi, z, \theta_r) g^{-1}(\phi, z, \theta_r) dz d\phi, \quad (1)$$

where μ_0 is vacuum permeability, r is the mean radius of the air gap, ϕ and z are angular and axial positions corresponding to an arbitrary point in the air gap and $g^{-1}(\phi, z, \theta_r)$ is the inverse of the air–gap function. For circuit "j" $n_j(\phi, z, \theta_r)$ and $N_j(\phi, z, \theta_r)$ are the "Winding Spatial Distribution" and the "Winding Modified Two-dimensional Function", respectively.

The latter can be expressed as,

$$N_j(\phi, z, \theta_r) = n_j(\phi, z, \theta_r) - 1/2\pi L \langle g^{-1}(\phi, z, \theta_r) \rangle \int_0^{2\pi} \int_0^L n_j(\phi, z, \theta_r)$$
$$g^{-1}(\phi, z, \theta_r) dz d\phi \quad (2)$$

where $\langle g^{-1}(\phi, z, \theta_r) \rangle$ is the mean value of the air–gap function inverse.

2.1. Calculation of inductances

From (1) and (2), it is possible to determine the coupling inductance between each circuit of the IM. One way to accomplish this is through expressing the winding functions by Fourier series. This also allows analyzing each spatial distribution harmonic separately. Below, the distribution of windings using Fourier series is widely discussed and the calculation of rotor and stator mutual inductances presented.

2.1.1. Windings distribution of stator and rotor circuits

Fig. 2 shows the distribution of the stator windings corresponding to phase a for a winding with full pitch and equal number of turns in all coils. In this figure, γ is the pitch and q is the number of coils per pole, N_t is the number of turns per phase and per pole and P is the number of pole pairs. The stator slots pitch γ is represented by,

$$\gamma = 2\pi/R_s, \quad (3)$$
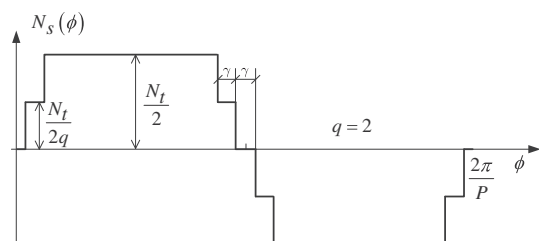
where R_s is the number of stator slots.

Fig. 2. Winding distribution. Particular case with $q = 2$.